

## Derin Su Yarı Batık Platformlarının Global Yorulma Analizi

Özgür Özgüç

ozguco@itu.edu.tr

İstanbul Teknik Üniversitesi, İstanbul, Türkiye

### ÖZET

Yarı batık açık deniz yapıları petrol ve doğal gaz sektöründe yaygın olarak kullanılır. Özellikle arama, sondaj, kurulum ve konaklama amaçlarında hizmet vermektedir. Derin ve sert sularda operasyon yapabilmek için dizayn edilirler. Yorulma, açık deniz çelik yapılar için kaçınılmaz problemlerden biri olarak bilinir. Tasarıma bağlı olarak, birçok bağlantı yapılarını içeren yarı batıklar özellikle yorulma yaralanmasına maruz kalırlar. Yorulma analizleri, tasarım aşamasında tekne yapısının yeterli bir yorulma mukavemetine sahip olması için detaylı bir şekilde yapılır. Bu çalışmanın temel amacı, derin su yarı-batık yapının yorulma hasarını hesaplamak ve yorulma ilişkili dizayn faktörleri ile birlikte yapısal bileşenleri dikkate alarak 40 ~ 400 yıl için ömür yeterliliğini teyit etmektir. Elde edilen sonuçlar özetlenip tartışmaya açılmıştır.

**Anahtar kelimeler:** Yorulma yaralanması, yarı batık yapıları, tekne yapısı, dinamik yükler, S-N eğrileri.

**Makale geçmişi:** Geliş 13/10/2018 – Kabul 25/11/2018

# Global Fatigue Assessment for Deepwater Semi-submersible Platform

Özgür Özgüç

ozguco@itu.edu.tr

Istanbul Technical University, Istanbul, Turkey

## ABSTRACT

Semi-submersible off-shore rigs are widely operated in offshore oil and gas industry, especially it serves the purpose of drilling, exploration, installation and accommodation purposes. It is designed for operating in deep waters and harsh environments. Fatigue damage is known as one of the unavoidable problems for offshore steel structures. Depending on the design type; a semi-submersible hull structure consists of connections that are prone to fatigue damage. Fatigue analyses should be carried out during the design stage so that the hull structure can have an adequate fatigue life. The main objective of this study is to calculate global fatigue damage and confirm the adequacy of the deepwater semi-submersible rig for 40 ~ 400 years life, where the structural components with respective design fatigue factors are accounted for. The results and insights derived from the present study are summarized and discussed.

**Keywords:** Fatigue damage, semi-submersible rig, hull structure, dynamic waves, S-N curves.

**Article history:** Received 13/10/2018 – Accepted 25/11/2018

## 1. Introduction

A semi-submersible is with minimum 20 years design life. The structure is exposed to environmental loads, payload, and changes of water ballast due to different operating conditions. The cyclic loads bring about possible fatigue problems and some of the critical locations which are considered sensitive to fatigue which are the connections between column – pontoon and column – brace. Every welded joint and structural detail or other form of stress concentration is a potential source of fatigue cracking and should be taken into consideration as well. Fatigue assessment which is supported by a detailed fatigue analyses are performed to make sure that the structure exposed to extensive dynamic loading has an adequate fatigue life and the estimated fatigue life obtained through analyses is used as a basic for planning inspection and maintenance program during the operation life of the structure.

Xie and Xie, 2009, focused on spectral-based fatigue analysis for offshore semi-submersible rig in South China Sea. The radiation/diffraction theory is used to calculate wave load acting on semi-submersible rig. The 3D FEA model of the rig is generated by using shell element, beam element, and mass element.

In accordance with long-term wave distribution of South China Sea, stress response of the global structure is determined. The fine FEA modelling of typical joint is performed, the result of global FEA is taken as the load boundary condition, and the hotspot stress transfer functions are calculated considering for hydrodynamic load and gravity load. Based on the Miner's rule, the fatigue life of the typical joint are determined by using a spectral fatigue analysis.

The fatigue life on key-components of semi-submersible platform is addressed by Jin et al., 2010 with spectral-based analysis. First of all, the stress responses of whole model platform under the random wave loads are determined. The calculation results of whole model platform for cut-boundary interpolation are generated in local model to calculate the key-component stress responses of the local model. Producing the fatigue stress energy spectrum by scaling the wave energy spectrum and the complex fatigue stress transfer function in detailed local model. The stress response of short-term sea-state is assumed to obey Rayleigh distribution, and the spectral moments are calculated. Finally, the fatigue life of key components is analyzed according to S-N curve and Palmgren-Miner's rule. The results show that the fatigue life of the connection meets the specification requirements, and the key elements are the fatigue sensitive areas of offshore semi-submersible rig.

Jin et al., 2016 addressed to analyse fatigue damage of an integrated structure model, where several methods are developed. An mixture simulation as well as a wind and wave coupling model are constructed to simulate combined wind and wave field accurately and efficiently. Formex algebra and the automatic replication technique are used to establish the parametric integrated model. The relationship between wind/wave and fatigue stress is presented to obtain the time histories of the hotspots' stresses. The fatigue damage of the hotspot is determined at different incident angles by using the rain flow counting method and Miner criterion. Some simulation results are expected to provide important reference for the wind and wave resistant designs in offshore platform design.

Before the oil price plunged from its peak in 2014, the growing demand for affordable and reliable energy especially fossil fuels has driven oil companies to invest in deep water exploration and drilling so as to tap the deep-water reserves. With the help of the technological advances, reserves in deep or ultra-deep water are now more accessible with drilling rigs that are specially designed for the water depth like semi-submersible rigs. Semi-submersibles are known with high payload and better stability with in terms of lesser rolling and pitching during drilling operations. In addition, global warming makes the Arctic and other icy regions more accessible for oil companies to carry out exploration and drilling in order to tap the possibly massive oil reserve in the region. Specially designed semi-submersibles that are able to work in arctic conditions seem to be attractive and practicable options for the possible massive oil and gas development in arctic region (Kok, 2017).

Kok, 2017 performed fatigue calculations on ring pontoon semi-submersibles, where two structural panel located on the pontoon-column connection points at the centre and side of the semi-submersible by using FE model with mesh size of 1cm x 1cm that are generated. Based on the assumptions and the loading condition considered, the adding of sponsons brings minor impact on the semi-submersible in terms of global responses, hydrodynamic load and fatigue life.

Ma and Yao, 2018, performed the fatigue lives of a new type of assembled marine floating platform for special purposes. Firstly, by using ANSYS AQWA software, the hydrodynamic model of the platform was established. Secondly, the structural stresses under alternating change loads were calculated under complex water environments, such as wind, wave, current and ice. The minimum fatigue lives were obtained under different working conditions. The analysis outcomes presented that the fatigue life of the rig structure can meet the requirements.

Ma et al., 2018 assessed fatigue damages on local components of a semi-submersible platform under combined actions of wind and wave loads in time domain. Some improvements are provided in the study to improve the efficiency and accuracy of the whole evaluating process. Firstly, a combined wind and wave relationship as well as an innovative mixture simulation method are used to generate time series of random wind and waves. Moreover, an m-block division method is proposed to compress the number of the complete short-term sea states in the wind-wave scatter diagram. Then, with an improved multiple interpolation sub-model method, the structural stress responses of the local structural components are calculated as is in the whole model analysis. Finally, a modified rain-flow counting method is provided and validated to count the stress cycles efficiently and accurately. Thus, the short- and long-term fatigue damages are computed based on the S-N curve approach and the cumulative fatigue damage rule. In relative agreement with the numerical results by the traditional time-domain method and existing experimental data, these proposed improved methods are demonstrated to be applicable and efficient methods for fatigue damage analyses.

Basically fatigue design is of increasing importance as the platforms are intended to design more cost-efficiently and for longer service. In ordinary ship and offshore structures such as oil tankers, FPSO, FLNG, drill-ships and the pontoons, the side shell is severely exposed to fatigue damages. The fatigue capacity of the side shell is strongly dependent on the local details design. Even small variations in the local design may significantly improve the fatigue capacity. The fatigue life is dependent on some factors such as global and local design, workmanship quality during construction, maintenance, corrosion protection, trade and load history. Offshore structures are subjected to variable cyclic loading during operation. Fatigue happens due to high stress concentrations around welds, and sharp geometric transitions at member connections. Fatigue crack starts at a localized spot and then with cyclic stress gradually increase over the cross section of the member.

Fatigue damages reduce the load-carrying capacity of the structure, and eventually may cause leakages, environmental pollutions, cargo mixing, contaminations or gas accumulating in enclosed spaces. In more serious cases, such structural damage may lead to catastrophic failure or even total loss of offshore units.

The main objective of this study is to calculate global fatigue damage and confirm the adequacy of the deepwater semi-submersible rig for 40 ~ 400 years life, where the structural components with respective design fatigue factors are accounted for.

## **2. Column Stabilized Semi-submersible Design**

The facility is a column-stabilised, offshore semi-submersible production unit supporting hydrocarbon processing systems and utilities, as well as living quarters for about 220 people.

The facility will be towed about 6,500 kilometres to the offshore Western Australia. It will be permanently moored near the field for the life of the project by 28 mooring lines, representing more than 27,000 tonnes of the anchor chain.

The main dimensions on the hull are given in Table 1 and Table 2 as follows.

**Table 1.** Main dimensions – General.

Operation draught (from keel)	26,00 m
Height, keel to underside Topsides BOS	48,00 m
Height, keel to main deck, TOS	62,00 m
Hull outer dimension excluding Guide Tube Box	110,30 m
Hull outer dimension including Guide Tube Box	118,675 m
Column spacing (centre to centre), (longitudinal and transverse)	83,65 x 83,65 m

**Table 2.** Main dimensions – Columns (rectangular types).

Number of columns	4
Width	26,65 m
Corner radius	6,20 m
Height from keel to top of column	48,00 m
Number of columns	4

A computerized hull structural and finite element (FE) models are demonstrated in Figure 1 and Figure 2.

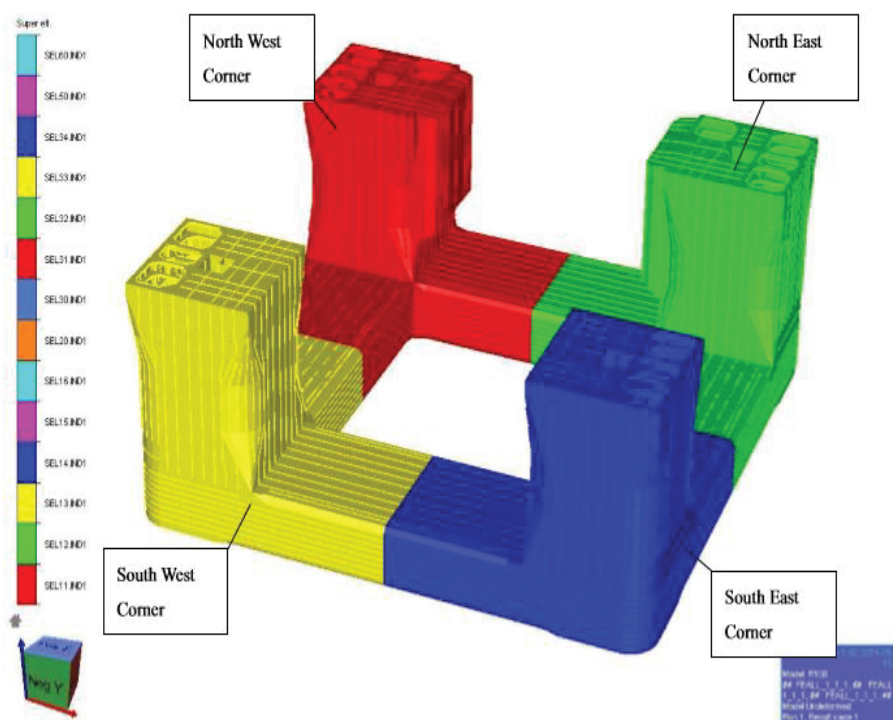


**Figure 1.** Hull main dimensions.

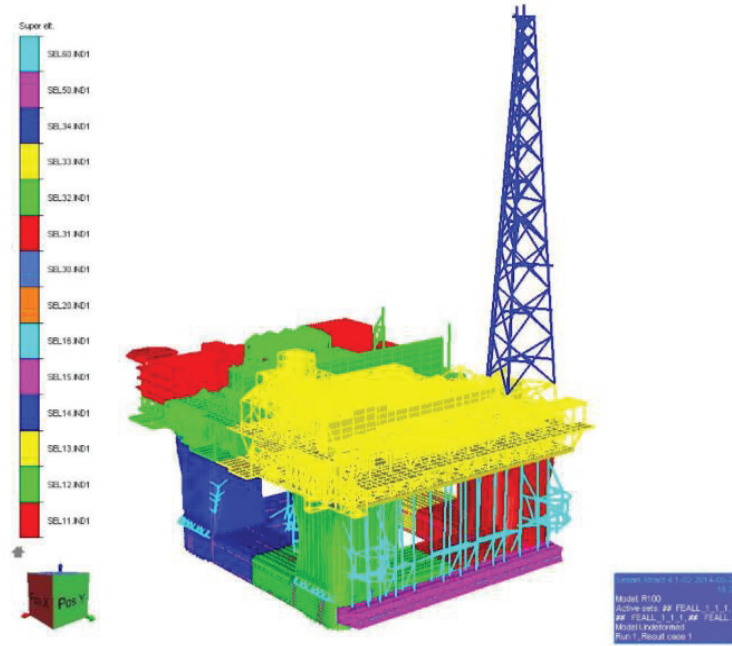


**Figure 2.** Computer finite element (FE) model.

The four-node shell element, three-node shell element, beam element and rod element are used for the Finite Element (FE) model. The unit for length and force is m and N respectively. When calculating the fatigue damage, the unit of stress is converted to MPa (N/mm<sup>2</sup>). The material density and Young's modulus are 7.85E3 kg/m<sup>3</sup> and 2.1E11 N/m<sup>2</sup> respectively.

FE models are generated based on gross scantling, which is sum of net scantling and DNV Class corrosion margin. The whole platform FE model with one longitudinal stiffener mesh is used for the global fatigue analysis such as typical element size are 600 mm.

### 3. Fatigue Cumulative Damage

The fatigue life may be calculated based on the S-N fatigue approach under the assumption of linear cumulative damage (Palmgrens-Miner rule).

When the long-term stress range distribution is expressed by a stress histogram, consisting of a convenient number of constant amplitude stress range blocks  $\Delta\sigma_i$  each with a number of stress repetitions  $n_i$  the fatigue criterion reads (DNVGL-RP-C203, 2010);

$$D = \sum_{i=1}^k \frac{n_i}{N_i} = \frac{1}{\bar{a}} \sum_{i=1}^k n_i \cdot (\Delta\sigma_i)^m \leq \eta \quad (1)$$

Where,

$D$  = accumulated fatigue damage

$\bar{a}, m$  = S-N fatigue parameters

$k$  = number of stress blocks

$n_i$  = number of stress cycles in stress block  $i$

$N_i$  = number of cycles to failure at constant stress range  $\Delta\sigma_i$

$\eta$  = usage factor. Accepted usage factor is defined as  $\eta = 1.0$

Applying a histogram to express the stress distribution, the number of stress blocks,  $k$ , is to be large enough to ensure reasonable numerical accuracy, and should not be less than 20. Due consideration should be given to selection of integration method as the position of the integration points may have a significant influence on the calculated fatigue life dependent on integration method (DNVGL-RP-C206, 2012).

When the long-term stress range distribution is defined by applying Weibull distributions for the different load conditions, and a one-slope S-N curves is used, the fatigue damage is given by,

$$D = \frac{v_0 T_d}{\bar{a}} \sum_{n=1}^{N_{load}} p_n q_n^m \Gamma\left(1 + \frac{m}{h_n}\right) \leq \eta \quad (2)$$

Where,

- $N_{load}$  = total number load conditions considered
- $p_n$  = fraction of design life in load condition  $n$ ,  $\sum p_n \leq 1$ , but normally not less than 0.85
- $T_d$  = design life of ship in seconds ( 20 years =  $6.3 \times 10^8$  sec. )
- $h_n$  = Weibull stress range shape distribution parameter for load condition  $n$ ,
- $q_n$  = Weibull stress range scale distribution parameter for load condition  $n$
- $v_0$  = long-term average response zero-crossing frequency
- $\Gamma\left(1 + \frac{m}{h_n}\right)$  = gamma function.

The Weibull scale parameter is defined from the stress range level,  $\Delta\sigma_0$ , as,

$$q_n = \frac{\Delta\sigma_0}{(\ln n_0)^{1/h_n}} \quad (3)$$

where  $n_0$  is the number of cycles over the time period for which the stress range level  $\Delta\sigma_0$  is defined. ( $\Delta\sigma_0$  includes mean stress effect) the zero-crossing-frequency may be taken as,

$$v_0 = \frac{1}{4 \cdot \log_{10}(L)} \quad (4)$$

where  $L$  is the ship rule length in meters.

Alternatively, in combination with calculation of stress range  $\Delta\sigma_0$  by direct analyses, the average zero crossing frequency.

When the long term stress range distribution is defined through a short term Rayleigh distribution within each short term period for the different loading conditions, and a one-slope S-N curve is used, the fatigue criterion reads as,

$$D = \frac{v_0 T_d}{\bar{a}} \Gamma\left(1 + \frac{m}{2}\right) \sum_{n=1}^{N_{load}} p_n \cdot \sum_{\substack{\text{all seastates} \\ \text{all headings}}} r_{ijn} (2\sqrt{2m_{0ijn}})^m \leq \eta \quad (5)$$

Where,

- $r_{ij}$  = the relative number of stress cycles in short-term condition  $i, j$
- $v_0$  = long-term average response zero-crossing-frequency,

$m_{0j}$  = zero spectral moment of stress response process

The Gamma function,  $\Gamma(1 + \frac{m}{2})$  is equal to 1.33 for  $m = 3.0$ .

The aim of the study and the literature review should be given in detail in the introduction section, with or without subheadings.

### 3.1. S-N Curve

The fatigue design is based on use of S-N curves that are obtained from fatigue tests. The design S-N curves which follow are based on the mean-minus-two-standard-deviation curves for relevant experimental data. The S-N curves are thus associated with a 97.6% probability of survival.

The S-N curves are applicable for normal and high strength steels used in construction of hull structures.

The basic design S-N curve is given as,

$$\log N = \log \bar{a} - m \log \Delta \sigma \quad (6)$$

Where,

$N$  = predicted number of cycles to failure for stress range  $\Delta \sigma$

$\Delta \sigma$  = stress range

$m$  = negative inverse slope of S-N curve

$\log \bar{a}$  = intercept of  $\log N$ -axis by S-N curve

$$\log \bar{a} = \log a - 2s \quad (7)$$

Where,

$a$  = is constant relating to mean S-N curve

$s$  = standard deviation of  $\log N$ ;

$s = 0.20$

S-N Curve F3 is used in the fatigue damage calculations and given in Table 3 and Table 4.

**Table 3.** S-N Curve in Air (DNVGL-RP-C203, 2010).

Table 2-1 S-N curves in air						
S-N curve	$N \leq 10^7$ cycles		$N > 10^7$ cycles $\log \bar{a}_2$ $m_2 = 5.0$	Fatigue limit at $10^7$ cycles *)	Thickness exponent $k$	Stress concentration in the S-N detail as derived by the hot spot method
	$m_1$	$\log \bar{a}_1$				
B1	4.0	15.117	17.146	106.97	0	
B2	4.0	14.885	16.856	93.59	0	
C	3.0	12.592	16.320	73.10	0.15	
C1	3.0	12.449	16.081	65.50	0.15	
C2	3.0	12.301	15.835	58.48	0.15	
D	3.0	12.164	15.606	52.63	0.20	1.00
E	3.0	12.010	15.350	46.78	0.20	1.13
F	3.0	11.855	15.091	41.52	0.25	1.27
F1	3.0	11.699	14.832	36.84	0.25	1.43
F3	3.0	11.546	14.576	32.75	0.25	1.61
G	3.0	11.398	14.330	29.24	0.25	1.80
W1	3.0	11.261	14.101	26.32	0.25	2.00
W2	3.0	11.107	13.845	23.39	0.25	2.25
W3	3.0	10.970	13.617	21.05	0.25	2.50
T	3.0	12.164	15.606	52.63	0.25 for SCF $\leq$ 10.0 0.30 for SCF $>$ 10.0	1.00

\*) see also section 2.10

**Table 4.** S-N Curve in Seawater with cathodic protection (DNVGL-RP-C203, 2010).

Table 2-2 S-N curves in seawater with cathodic protection						
S-N curve	$N \leq 10^6$ cycles		$N > 10^6$ cycles $\log \bar{a}_2$ $m_2 = 5.0$	Fatigue limit at $10^7$ cycles <sup>*)</sup>	Thickness exponent $k$	Stress concentration in the S-N detail as derived by the hot spot method
	$m_1$	$\log \bar{a}_1$				
B1	4.0	14.917	17.146	106.97	0	
B2	4.0	14.685	16.856	93.59	0	
C	3.0	12.192	16.320	73.10	0.15	
C1	3.0	12.049	16.081	65.50	0.15	
C2	3.0	11.901	15.835	58.48	0.15	
D	3.0	11.764	15.606	52.63	0.20	1.00
E	3.0	11.610	15.350	46.78	0.20	1.13
F	3.0	11.455	15.091	41.52	0.25	1.27
F1	3.0	11.299	14.832	36.84	0.25	1.43
F3	3.0	11.146	14.576	32.75	0.25	1.61
G	3.0	10.998	14.330	29.24	0.25	1.80
W1	3.0	10.861	14.101	26.32	0.25	2.00
W2	3.0	10.707	13.845	23.39	0.25	2.25
W3	3.0	10.570	13.617	21.05	0.25	2.50
T	3.0	11.764	15.606	52.63	0.25 for SCF $\leq$ 10.0 0.30 for SCF $>$ 10.0	1.00

<sup>\*)</sup> see also 2.10

#### 4. Fatigue Damage Assessment Procedure

The analysed model includes the hull and topside structure. Results for main elements of hull are presented in this study. The global dynamics analysis returns the 200 years stress amplitude for operating and  $10^{-5}$  probability stress amplitude for towing condition. The loading consists of global extreme design wave loads with 200 years return period for operating condition and  $10^{-5}$  probability for towing condition respectively. The direction of the design waves are chosen to give the maximum response at various locations on the platform (DNVGL-OS-C103, 2015).

Stochastic fatigue analysis is performed in order to calculate the fatigue damage of the hull. Global model loading includes unit waves, hydrodynamic loads and accelerations due to platform motions. The long-term stress distribution is obtained by multiplying chosen wave spectra and scatter diagram with the principal stress transfer functions obtained from the dynamic wave response analysis (DNVGL-OS-C101, 2016).

Additionally, the damage (Miner-Palmgren rule) due to long-term stress distribution will be calculated with specific S-N curve, DFF and SCF. Stress points are taken into the element corner points. The shell element top and bottom sides were put into consideration when extracting principal stresses and damage. The dynamic wave response analysis is performed by using WADAM, which provides input to the structural analysis in forms of hydrodynamics forces and inertia forces. SESTRAS is used for structural analysis and fatigue damage is calculated by STOFAT module (DNV SESAM, 2011).

Semi-submersible platform is designed to withstand a total of 40 years' life duration taking into account on-site and towing loading from shipyard to on-site. Following flow diagram for global fatigue calculation is provided in Figure 3, where how those parameters are used and implemented in the fatigue assessment. Corresponding number of cycles and critical stress are also referred to corresponding to S-N Curves given by DNV-OS-C203 Standard.

In the global model that typical element size are 600 mm. Even if 8noded elements are used, the results from the FE analysis are to be considered as nominal stress because the elements are too big to give

realistic stress concentrations in the hotspot detail. The stresses must be scaled with a geometrical SCF before fatigue damage is calculated. Magnitude SCF is depending on the detail.

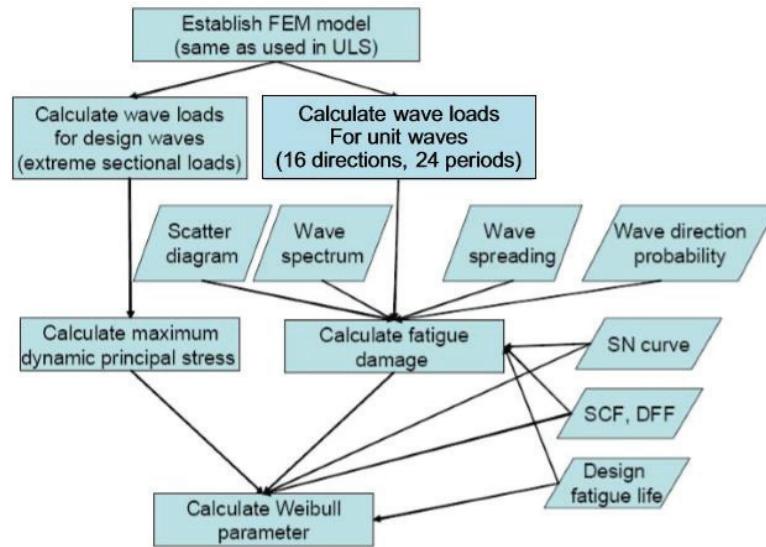


Figure 3. Flow diagram for global fatigue calculation.

Solution (displacements) of the global analysis is transferred to the local models using submodelling technique. The idea of submodelling is in general that a portion of a global model is separated from the rest of the structure, re-meshed and analyzed in greater detail. The calculated deformations from the global analysis are applied as boundary conditions on the borders of sub models.

### 5. Fatigue Input for Operating Condition

Omnidirectional Hs-Tp scatter diagram with wave spreading (short-crested seas) have been used as shown in the following Table. The JONSWAP wave spectrum has been used for parameterizing sea states in the scatter diagram.

Cos8 wave spreading is used for accounting wave spreading which corresponding to a wave-spread factor of 0.9. Wave loads are generated in WADAM (DNV Sesam, 2011) and after stiffness analysis; the fatigue damage is calculated by using STOFAT. In the analysis the following 24 wave periods varying from 0.8 ~ 2.1 rad/s (equivalent to 3 to 35 seconds) and 16 wave directions have been accounted for.

Table 5. S-N Curve in Seawater with cathodic protection (DNVGL-RP-C203, 2010).

Wave Direction (degree)	Wave Periods (rad/s)																							
	0.18	0.2	0.25	0.3	0.35	0.4	0.45	0.5	0.55	0.6	0.65	0.7	0.75	0.8	0.85	0.9	1.0	1.1	1.2	1.3	1.4	1.6	1.8	2.1
0	0.18	0.2	0.25	0.3	0.35	0.4	0.45	0.5	0.55	0.6	0.65	0.7	0.75	0.8	0.85	0.9	1.0	1.1	1.2	1.3	1.4	1.6	1.8	2.1
22.5	0.18	0.2	0.25	0.3	0.35	0.4	0.45	0.5	0.55	0.6	0.65	0.7	0.75	0.8	0.85	0.9	1.0	1.1	1.2	1.3	1.4	1.6	1.8	2.1
45	0.18	0.2	0.25	0.3	0.35	0.4	0.45	0.5	0.55	0.6	0.65	0.7	0.75	0.8	0.85	0.9	1.0	1.1	1.2	1.3	1.4	1.6	1.8	2.1
67.5	0.18	0.2	0.25	0.3	0.35	0.4	0.45	0.5	0.55	0.6	0.65	0.7	0.75	0.8	0.85	0.9	1.0	1.1	1.2	1.3	1.4	1.6	1.8	2.1
90	0.18	0.2	0.25	0.3	0.35	0.4	0.45	0.5	0.55	0.6	0.65	0.7	0.75	0.8	0.85	0.9	1.0	1.1	1.2	1.3	1.4	1.6	1.8	2.1
112.5	0.18	0.2	0.25	0.3	0.35	0.4	0.45	0.5	0.55	0.6	0.65	0.7	0.75	0.8	0.85	0.9	1.0	1.1	1.2	1.3	1.4	1.6	1.8	2.1
135	0.18	0.2	0.25	0.3	0.35	0.4	0.45	0.5	0.55	0.6	0.65	0.7	0.75	0.8	0.85	0.9	1.0	1.1	1.2	1.3	1.4	1.6	1.8	2.1
157.5	0.18	0.2	0.25	0.3	0.35	0.4	0.45	0.5	0.55	0.6	0.65	0.7	0.75	0.8	0.85	0.9	1.0	1.1	1.2	1.3	1.4	1.6	1.8	2.1
180	0.18	0.2	0.25	0.3	0.35	0.4	0.45	0.5	0.55	0.6	0.65	0.7	0.75	0.8	0.85	0.9	1.0	1.1	1.2	1.3	1.4	1.6	1.8	2.1
202.5	0.18	0.2	0.25	0.3	0.35	0.4	0.45	0.5	0.55	0.6	0.65	0.7	0.75	0.8	0.85	0.9	1.0	1.1	1.2	1.3	1.4	1.6	1.8	2.1
225	0.18	0.2	0.25	0.3	0.35	0.4	0.45	0.5	0.55	0.6	0.65	0.7	0.75	0.8	0.85	0.9	1.0	1.1	1.2	1.3	1.4	1.6	1.8	2.1
247.5	0.18	0.2	0.25	0.3	0.35	0.4	0.45	0.5	0.55	0.6	0.65	0.7	0.75	0.8	0.85	0.9	1.0	1.1	1.2	1.3	1.4	1.6	1.8	2.1
270	0.18	0.2	0.25	0.3	0.35	0.4	0.45	0.5	0.55	0.6	0.65	0.7	0.75	0.8	0.85	0.9	1.0	1.1	1.2	1.3	1.4	1.6	1.8	2.1
292.5	0.18	0.2	0.25	0.3	0.35	0.4	0.45	0.5	0.55	0.6	0.65	0.7	0.75	0.8	0.85	0.9	1.0	1.1	1.2	1.3	1.4	1.6	1.8	2.1
315	0.18	0.2	0.25	0.3	0.35	0.4	0.45	0.5	0.55	0.6	0.65	0.7	0.75	0.8	0.85	0.9	1.0	1.1	1.2	1.3	1.4	1.6	1.8	2.1
337.5	0.18	0.2	0.25	0.3	0.35	0.4	0.45	0.5	0.55	0.6	0.65	0.7	0.75	0.8	0.85	0.9	1.0	1.1	1.2	1.3	1.4	1.6	1.8	2.1

The stochastic fatigue analysis is performed with S-N F3 curve for seawater with cathodic protection (DNVGL-RP-C203, 2010), where the unit waves are presented in Table 5.

### 6. Fatigue Input for Towing Condition

The fatigue damage for towing is calculated by using wave scatter from Korea to Australia as given in Table 6. Total towing duration is assumed 38 days with towing speed 3.5 knots of average speed. Wave scatter for each sail away scenario will be made under the duration time at each location, season and probability of sea state (DNV-RP-F205, 2010).

**Table 6.** Transit Route D from Korea to Australia – Speed 3.5 knots

Route D	Distance (nm)	Duration (38 day Base)	Duration (48 day Base)	No delay	1 month delay	2 month delay	3 month delay	4 month delay	5 month delay	6 month delay
WW1	271	3.2	<b>4.07</b>	Nov	<b>Dec</b>	Jan	Feb	Mar	Apr	May
WW2	240	2.9	<b>3.69</b>	Nov	<b>Dec</b>	Jan	Feb	Mar	Apr	May
WW3	301	3.6	<b>4.58</b>	Dec	<b>Jan</b>	Feb	Mar	Apr	May	Jun
WW4	300	3.6	<b>4.58</b>	Dec	<b>Jan</b>	Feb	Mar	Apr	May	Jun
WW5	330	3.9	<b>4.97</b>	Dec	<b>Jan</b>	Feb	Mar	Apr	May	Jun
WW6	662	7.9	<b>10.06</b>	Dec	<b>Jan</b>	Feb	Mar	Apr	May	Jun
WW7	568	6.8	<b>8.66</b>	Dec	<b>Jan</b>	Feb	Mar	Apr	May	Jun
WW8	292	3.5	<b>4.46</b>	Dec	<b>Jan</b>	Feb	Mar	Apr	May	Jun
Ichthys	189	2.3	<b>2.93</b>	Dec	<b>Jan</b>	Feb	Mar	Apr	May	Jun
<b>Total</b>	<b>3,153</b>	<b>38</b>	<b>48</b>							

Wave scatter for each sail away scenario will be made under the duration time at each location, season, and probability of sea state. JONSWAP peakedness parameters based on DNV simplified method are summarized in below Table 9. JONSWAP peakedness parameters based on DNV simplified method. Most of the peakedness parameters for the sea state over 5% probability are below 2.0. Therefore, JONSWAP peakedness parameter 2.0 shall be used in towing fatigue analysis. Wave scatter for 1-month delay sail away case is shown in Table 7. An example of combined wave scatter is shown below in Table 8.

**Table 7.** Wave scatter for 1-month delay sail away case.

Hs[m]	Tp [sec]											Total
	1	3	5	7	9	11	13	15	17	19	21	
0.25		2.884	<b>6.758</b>	0.774	1.098	1.934	1.114	0.147	0.027			14.735
0.75		3.795	<b>7.591</b>	1.861	0.983	1.634	1.406	0.232	0.065	0.008		17.577
1.25		0.204	<b>6.519</b>	<b>5.569</b>	3.414	1.099	0.576	0.192	0.023			17.595
1.75			3.639	<b>7.333</b>	<b>5.817</b>	1.048	0.344	0.082	0.021			18.285
2.25		0.001	0.737	<b>6.186</b>	<b>5.342</b>	0.852	0.177	0.044	0.008			13.347
2.75			0.037	3.290	3.666	0.581	0.130	0.012				7.715
3.25				1.695	2.440	0.637	0.029	0.007				4.809
3.75				0.487	1.868	0.298	0.006	0.004				2.663
4.25				0.086	1.307	0.206	0.000					1.599
4.75				0.002	0.692	0.167	0.000					0.862
5.25					0.301	0.120	0.002					0.422
5.75					0.091	0.110	0.001					0.202
6.25					0.014	0.164	0.014					0.192
<b>Total</b>	<b>0.000</b>	<b>6.885</b>	<b>25.281</b>	<b>27.284</b>	<b>27.033</b>	<b>8.849</b>	<b>3.800</b>	<b>0.719</b>	<b>0.144</b>	<b>0.008</b>	<b>0.000</b>	<b>100.002</b>

**Table 8.** Combined wave scatter.

Wave scatter for area 1			Wave scatter for area 2		
Hs / Tp	1 sec	2 sec	Hs / Tp	1 sec	2 sec
0.5m	0.1	0.4	0.5m	0.05	0.15
1.0m	0.2	0.3	1.0m	0.3	0.5
Duration (day)	3		Duration (day)	7	

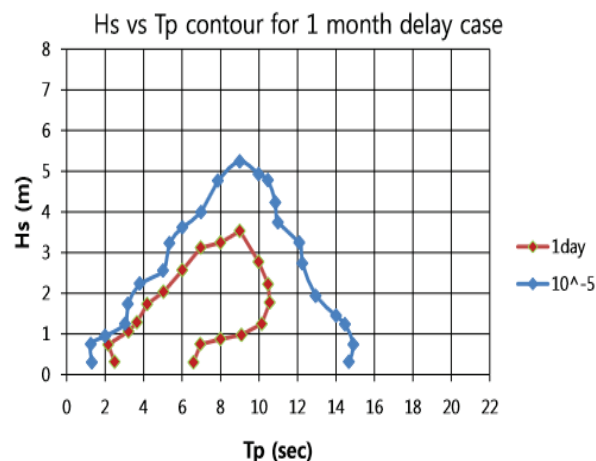
  

Combined wave scatter		
Hs / Tp	1 sec	2 sec
0.5m	0.1 x 3 + 0.05 x 7	0.4 x 3 + 0.15 x 7
1.0m	0.2 x 3 + 0.3 x 7	0.3 x 3 + 0.5 x 7
Duration (day)	10	

The most severe wave scatter data among 7 scenarios described in below Table 9 is 1 month delay case (=2 month delay case) based on wave energy ( $H^2 \times \text{probability}$ ). The wave scatter for 1 month delay case will be used for towing fatigue analysis.  $H_s - T_p$  contours for  $10^{-5}$  probability level are considered in towing design wave condition for simplified fatigue analysis (DNVGL-RP-C206, 2012) and presented in Figure 4. It is obtained from the above wave scatter diagram data and shown below in Table 9.

**Table 9.** JONSWAP peakedness parameters based on DNV simplified method (DNV-OS-C206, 2012).

Hs [m]	Tp [sec]										
	1	3	5	7	9	11	13	15	17	19	21
0.25		1.00	1.00	1.00	1.00	1.00	1.00	1.00	1.00		
0.75		5.00	1.00	1.00	1.00	1.00	1.00	1.00	1.00	1.00	
1.25		5.00	1.83	1.00	1.00	1.00	1.00	1.00	1.00		
1.75			4.07	1.00	1.00	1.00	1.00	1.00	1.00		
2.25		5.00	5.00	1.47	1.00	1.00	1.00	1.00	1.00		
2.75			5.00	2.45	1.00	1.00	1.00	1.00			
3.25				3.61	1.01	1.00	1.00	1.00			
3.75				4.92	1.50	1.00	1.00	1.00			
4.25				5.00	2.07	1.00	1.00				
4.75				5.00	2.72	1.00	1.00				
5.25					3.43	1.26	1.00				
5.75					4.19	1.61	1.00				
6.25					5.00	1.99	1.00				



**Figure 4.**  $H_s - T_p$  contours for 1 month delay case for towing state.

## 7. Loads

**Table 10.** Load cases for 200 years return period for operating conditions.

Complex load no	Parameter	Wave heading (deg.)	Wave period (sec)	Wave amplitude (m)	Response
					90% fractile
CL1	Longitudinal Split Force	0	11.5	8.41	215.83 [MN]
CL2	Transverse Split Force	270	11.5	8.50	228.55 [MN]
CL3	Roll Connection Moment	330	8.0	4.26	2375.77 [MNm]
CL4	Pitch Connection Moment	60	8.0	3.04	1970.07 [MNm]
CL5	Longitudinal Shear Force	315	8.0	7.76	66.92 [MN]
CL6	Longitudinal Shear Force	315	11.5	9.7	66.92 [MN]
CL7	Transverse Shear Force	225	8.0	7.87	69.49 [MN]
CL8	Transverse Shear Force	225	11.0	9.62	69.49 [MN]
CL9	Longitudinal Racking Force	180	8.0	5.53	0.94 [m/s <sup>2</sup> ]
CL10	Transverse Racking Force	270	8.0	5.47	0.98 [m/s <sup>2</sup> ]
CL11	Vertical Racking Force	0	13.5	9.76	1.28 [m/s <sup>2</sup> ]
CL12	Longitudinal Split Force	30	11.5	8.62	152.31 [MN]
CL13	Longitudinal Split Force	210	11.5	8.72	152.35 [MN]
CL14	Transverse Split Force	300	12.0	8.61	163.66 [MN]
CL15	Transverse Split Force	240	12.0	8.61	163.05 [MN]

**Table 11.** Load cases for 10<sup>5</sup> probability for towing conditions (at 15m draft).

Complex load no	Parameter	Wave heading (deg.)	Wave period (sec)	Wave amplitude (m)	Response
					90% fractile
CL1	Longitudinal Split Force	0	11.5	8.41	215.83 [MN]
CL2	Transverse Split Force	270	11.5	8.50	228.55 [MN]
CL3	Roll Connection Moment	330	8.0	4.26	2375.77 [MNm]
CL4	Pitch Connection Moment	60	8.0	3.04	1970.07 [MNm]
CL5	Longitudinal Shear Force	315	8.0	7.76	66.92 [MN]
CL6	Longitudinal Shear Force	315	11.5	9.7	66.92 [MN]
CL7	Transverse Shear Force	225	8.0	7.87	69.49 [MN]
CL8	Transverse Shear Force	225	11.0	9.62	69.49 [MN]
CL9	Longitudinal Racking Force	180	8.0	5.53	0.94 [m/s <sup>2</sup> ]
CL10	Transverse Racking Force	270	8.0	5.47	0.98 [m/s <sup>2</sup> ]
CL11	Vertical Racking Force	0	13.5	9.76	1.28 [m/s <sup>2</sup> ]
CL12	Longitudinal Split Force	30	11.5	8.62	152.31 [MN]
CL13	Longitudinal Split Force	210	11.5	8.72	152.35 [MN]
CL14	Transverse Split Force	300	12.0	8.61	163.66 [MN]
CL15	Transverse Split Force	240	12.0	8.61	163.05 [MN]

The maximum dynamic stresses have been calculated by using design waves as shown in the Table 10 and Table 11 as above. Only the maximum hogging and sagging ballast condition have been accounted for (DNV-RP-C205, 2014).

## 8. Results and Discussion

The main purpose of this study is to calculate global fatigue limit state (FLS) and confirm the adequacy of the deepwater semi-submersible rig for 40 ~ 400 years life for the structural components with respective design fatigue factors. The computer model consist of all structural members such as all main bearing elements, columns, nodes and pontoons in the hull are modelled with shell elements for webs and beam element for flanges. Stiffeners are lumped and modelled as beam elements with correct sectional areas.

Ballast water is distributed in pontoons in such way that maximum hogging and sagging conditions are simulated. This is achieved by filling one pontoon and keeping one pontoon empty. Two analyses have been run; one dynamic analysis and one stochastic fatigue analysis. The global dynamic analysis returns the 200 years stress amplitude for operating and  $10^{-5}$  probability stress amplitude for towing condition. The loading consists of global extreme design wave loads with 200 years return period for operating condition and  $10^{-5}$  probability for towing condition respectively.

The fatigue damage is calculated by using a stochastic analysis based on a long term wave statistics (DNVGL-RP-C203, 2010). An omni-directional scatter diagram is used. Directional probabilities for 16 evenly spaced wave directions are used. Totally 24 wave periods varying from 0.18 ~ 2.1 rad/s (equivalent to 3 to 35 seconds) are used. For towing condition, combined wave scatter diagram is considered according to the towing route from Korea to Australia and departure scenarios. 1 month delay case is the most severe scenario and it is taken into account in towing fatigue analysis (DNV STOFAT, 2011).

The conclusions can be drawn such as the fatigue damage is below 0.4 except for the areas around the castings in operating condition as shown in Figure 5 while the fatigue damage is below 0.4 except for the areas around the castings in towing condition as presented in Figure 6.

Figure 5 and Figure 6 show the stochastic fatigue analysis using global model. Noticed that fatigue life higher than the minimum required design life of at least 40 years such as the pontoon-column connection facing inwards (Figure 5) and those on the side shells that facing outboard (Figure 6) which are the critical areas. The fatigue life is 40 years and above.

Figure 5 shows the fatigue usage factor of the global model. Noticed that the whole model is with very low usage factor except that for critical such as the connection between pontoon/column, the usage factor is close to 0.4. Figure 6 shows the expected fatigue life for the model. Noticed that all locations are with fatigue life of at least above 40 years. As the design life is only 40 years, thus the structure is with fatigue design factor  $>10$  except the connection point and a few other locations.

In overall, the analysis results show that in particular the major intersections of pontoon / column of a typical ring pontoon unit are sensitive to the fatigue cracking, such as,

- centre bulkhead pontoon / column intersection at pontoon upper deck
- pontoon outer wall / column intersection at pontoon upper deck
- pontoon / pontoon intersections.

The wave loads fatigue damage is calculated assuming it follows Rayleigh distribution. However, other load components that have different distribution, fatigue damage should be calculated in different way and total fatigue damage is calculated by summing up damage from each load component. Besides wave induced loads, following load components should also be considered in the future work.

- Low Cycle Loads due to Cargo Loading/Offloading,
- Wind Loads,
- 2<sup>nd</sup> order slowly drifting forces.

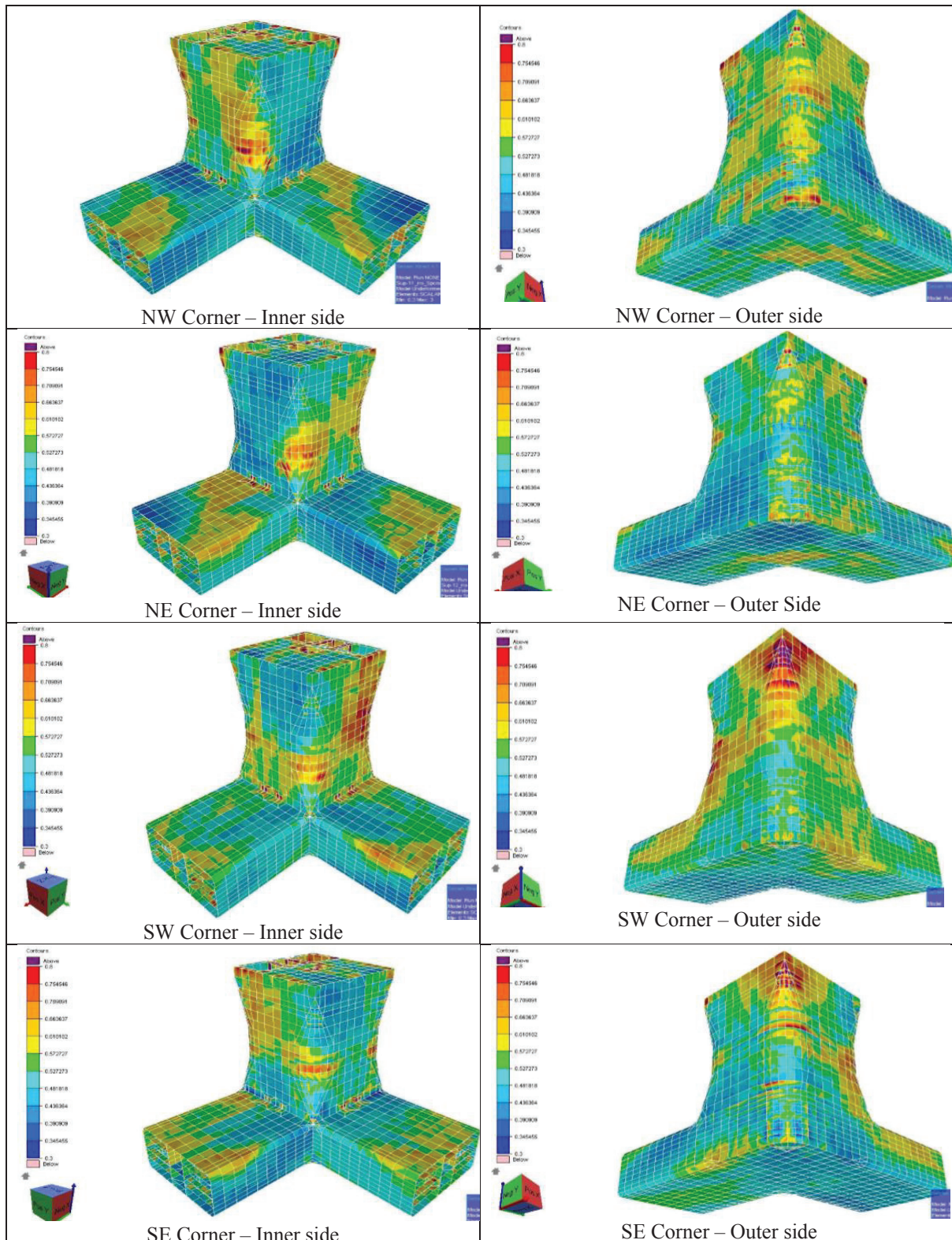


**Figure 5.** Calculated fatigue damage for operating condition.

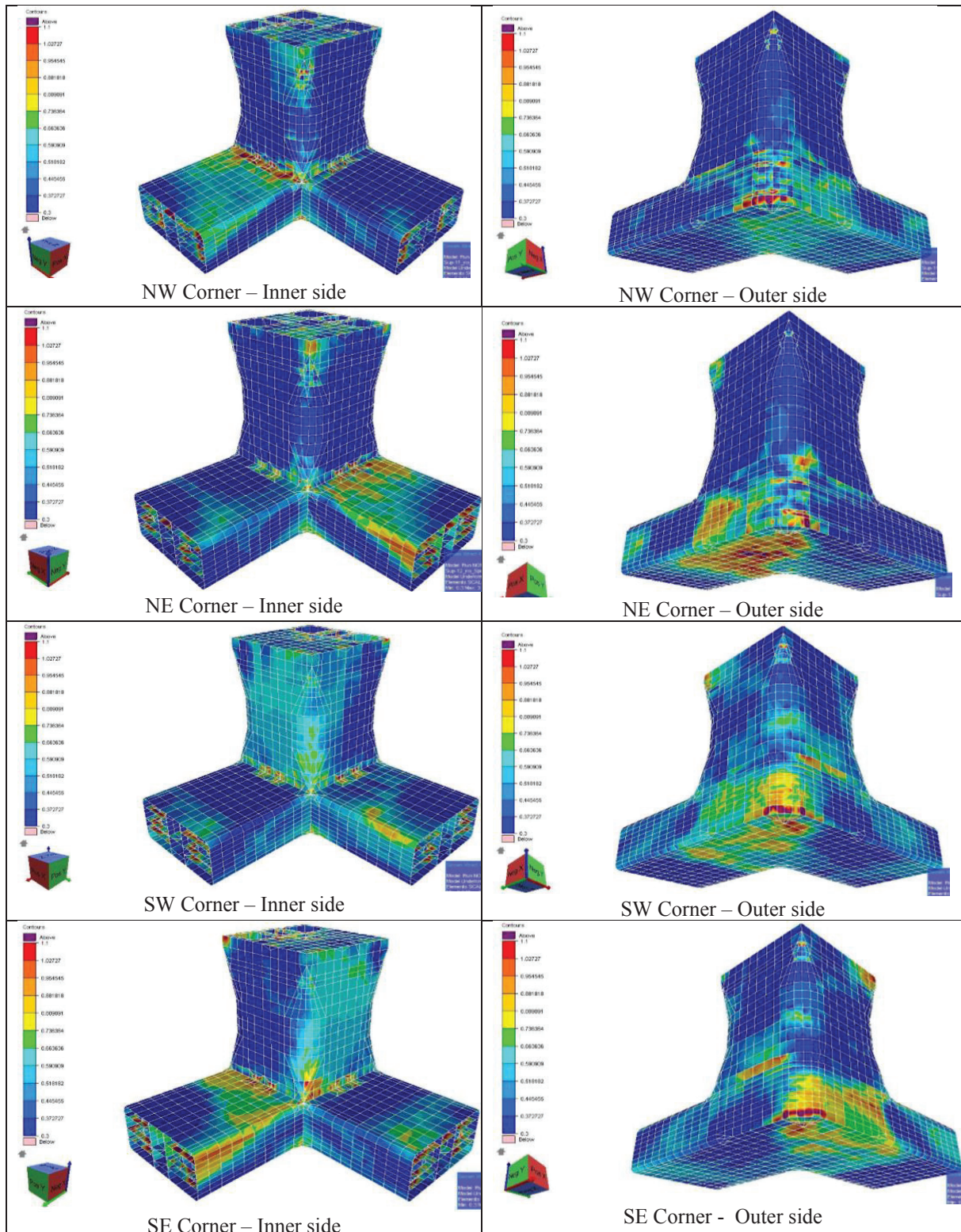


**Figure 6.** Calculated fatigue damage for towing condition.

Wind load or 2<sup>nd</sup> order drifting force is related to details in offshore area. Therefore, only low cycle loads from cargo loading/unloading should also be considered as non-wave frequency loads in fatigue damage assessment of semi-submersible hull structure.

## 9. References

- Cui, L., Xu, J., He, Y., and Jin, W. (2010). Fatigue Analysis on Key Components of Semi-Submersible Platform. ASME. International Conference on Offshore Mechanics and Arctic Engineering, 29th International Conference on Ocean, Offshore and Arctic Engineering, Volume 2:671-675.
- DNV-GL (2015). DNVGL-OS-C103, Structural Design of Column Stabilised Units - LRFD method.
- DNV (2011). Sesam User Manual.
- DNV (2010). DNV-RP-F205, Global Performance Analysis of Deep Water Floating Structure.
- DNV-GL (2016). DNVGL-OS-C101, Design of Offshore Steel Structures - LRFD Method.
- DNV (2014). DNV-RP-C205, Environmental Conditions and Environmental Loads.
- DNV-GL (2012). DNVGL-RP-C206, Fatigue Methodology of Offshore Ships.
- DNV-GL (2010). DNVGL-RP-C203, Fatigue Design of Offshore Steel Structure.
- DNV (2011). Fatigue Assessment Using SESAM Program Modules Stofat, Framework and Postresp.
- Kok, Y.G. (2017). Fatigue Analysis of Semi-submersible, Master Thesis, West Pomeranian University of Technology, Szczecin.
- Ma, G and Yao, Y. (2018). Fatigue Analysis of Assembled Marine Floating Platform for Special Purposes under Complex Water Environments, IOP Conf. Ser.: Earth Environ. Sci. 128 012062.
- Ma, J., Zhoi, D., Pan, X., and Zhu, H. (2016). Proceedings of IASS Annual Symposia, IASS 2016 Tokyo Symposium: Spatial Structures in the 21st Century – Computational Methods, pp. 1-10(10).
- Ma, J., Zhou, D., Bao, Y., and Han, Z. (2018). Fatigue Assessment on Local Components of a Semi-submersible Platform Subjected to Wind and Wave Loads, Journal of Vibroengineering, Vol. 20, Issue 2, pp. 988-1006.
- Xie, B. and Xie, W. (2009). Spectral-based Fatigue Analysis for Deepwater Semi-Submersible Rig in South China Sea, International Society of Offshore and Polar Engineers.
- [https://atlantis.udhb.gov.tr/istatistik/istatistik\\_kabotaj.aspx](https://atlantis.udhb.gov.tr/istatistik/istatistik_kabotaj.aspx) [Online] [Erişim 19.02.2018]